Sensors & Transducers, Vol. 255, Issue 1, January 2022, pp. 1-9

Sensors & Transducers

Published by IFSA Publishing, S. L., 2022
http://www.sensorsportal.com

Polarization State Sensor Based on Polarization-Holographic Diffraction Element

Barbara KILOSANIDZE and George KAKAURIDZE
Georgian Technical University, Institute of Cybernetics,
Laboratory of Holographic Recording and Processing of Information,
5 Z. Anjaparidze Str., 1086 Tbilisi, Georgia
Tel.: + 995593306693
E-mail: b.kilosanidze@gtu.ge

Received: 4 December 2021 /Accepted: 10 January 2022 /Published: 31 January 2022

Abstract: An innovative polarization state sensor is presented for the determination of the distribution of polarization state of light reflected from the different objects. Such a sensor based on only one integral polarization-holographic diffraction element developed by us is used for real-time analysis of the polarization state of light. The simultaneous measurement of the intensities of four beams diffracted on the element and the appropriate software enable the complete polarization state of an analyzable light (the four Stokes parameters) to be obtained in real-time. The polarization state of light reflected from the object enables to obtain the physical-chemical characteristics of the object's surface. An application of the sensor in the tasks of remote sensing and in studying a stressed state in different constructions are presented. Such sensor has many advantages compared to conventional devices of polarization optics: operation in real time; a wide spectral range; they differ by compactness, universality, simplicity, light weight and comparative cheapness.

Keywords: Polarization state sensor, Diffraction and gratings, Polarization-holographic element, Polarimetry, Stokes parameters.

1. Introduction

The information capacity of the methods of determining the characteristics of the object essentially increases when together with other characteristics of light reflected from an object the polarization state is taken into account. In this case, the additional parameters of information processing are introduced (ellipticity, the azimuth, the direction of rotation, and the degree of polarization).

Information on the polarization state of light scattered or radiated by different objects plays an increasing role in remote sensing, ellipsometry, astropolarimetry, object recognition and others. Therefore, the development of simple, precision and real-time sensor for determining the polarization state and also the distribution of polarization state on the images of different objects without any scanning, taken into account also a dispersion of this distribution, is rather urgent.

The method of recording and reconstructing of the vector character of the fields of electromagnetic wave – polarization holography - was first proposed by Prof. Sh Kakichashvili in 1972 [1, 2].

One of the most promising applications of polarization holography is the creation of polarization-holographic gratings with different anisotropic-gyrotropic profile. Such gratings could be applied in various fields of science and engineering, where the analysis and transformation of light are necessary [3].

The polarization-holographic method gives the possibility to create polarization-holographic diffraction elements (PHE) which enables carrying out a complete analysis of the state and degree of polarization in real-time and working in a wide spectral range including near infra-red [3, 4]. We suggest an innovative sensor of the polarization state based on such an integral polarization-holographic element. Let us note that currently used sensors and polarimeters are complex and expensive devices and most of them contain mechanically rotating or electronically tunable optical elements [5, 6].

In this paper, the description and characteristics of the suggested polarization state sensor and the examples of its application in the tasks of remote sensing and in studying a stressed state in different constructions are presented.

2. Polarization-Holographic Diffraction Element

We suggest carrying out a complete real time analysis of the polarization state of light (also the distribution of the polarization state) by only one Integral Polarization-Holographic Diffraction Element. Such an element was created by means of polarization-holographic method, when some polarization-holographic gratings with different profile of the anisotropy and gyrotropy in the band are recorded on one and the same area of polarization-sensitive material, so that the beams diffracted on each hologram have been spatially separated [4, 7].

In [4] the general case of the recording of polarization-holographic gratings by two coherent beams of arbitrary elliptic polarization was considered. We have developed the theoretical model to describe the functioning of the sensor.

The Jones vectors [8] of the two recording beams are

$$\hat{\psi} = \begin{pmatrix} \psi_x \exp ia_x \\ \psi_y \exp ia_y \end{pmatrix} \exp i\omega t, \quad \hat{\xi} = \begin{pmatrix} \xi_x \exp ib_x \\ \xi_y \exp ib_y \end{pmatrix} \exp i(\omega t + \delta), \tag{1}$$

where $\hat{\psi}_x = \psi_x \exp ia_x$ and $\hat{\psi}_y = \psi_y \exp ia_y$, $\hat{\xi}_x = \xi_x \exp ib_x$ and $\hat{\xi}_y = \xi_y \exp ib_y$ are the x and y components of the complex amplitude of the two recording beams; ω is the frequency; and δ is the phase shift that occurs at a certain angle between the beams during recording.

We use polarization-sensitive materials for recording polarization-holographic gratings and elements on their basis. In such materials a photoanisotropy and photogyrotropy of optical parameters are induced under the action of polarized light. The side-chain polymers, the materials based on azodyes in polymer matrices and azodyes-colored liquid crystalline polymers are mostly used materials for polarization-holographic recording. The recording materials used by us are stable and due to this fact information recording on such materials is kept for a long time (some years and more) [9, 10].

The regularity of the connection of anisotropy and gyrotropy induced by polarized light with the polarization characteristics of the inducing light were obtained [11, 12]. This regularity is of universal character irrespective of the mechanism of anisotropy and gyrotropy induction. The complex coefficients of the photoinduced linear and circular birefringence appear in this regularity and functions of the scalar (isotropic) reaction $\hat{s}$ on the acting intensity of light and two vector reactions – the anisotropic reaction $\hat{v}_L$ on linearly polarized light and the gyrotropic reaction $\hat{v}_G$ on circularly polarized light are introduced to describe the photoresponse of the polarization-sensitive medium

$$\hat{n}_{1,2}^2 = \hat{n}_0^2 + \hat{s}(I_1 + I_2) \pm \sqrt{[\hat{v}_L(I_1 - I_2)]^2 + [\hat{v}_G(I^+ - I^-)]^2}, \tag{2}$$

where $\hat{n}_1$ and $\hat{n}_2$ are the complex coefficients of elliptical birefringence of the medium; $\hat{n}_0$ is the complex refractive index of the medium in the initial unirradiated state; a complex refractive index is given in the form of $\hat{n} = n - in\tau$ (n is the real refractive index and τ is the extinction coefficient); $I_1 + I_2$ is the first Stokes parameter, $I_1 - I_2$ is the second Stokes parameter, and $I^+ - I^-$ is the fourth Stokes parameter of the inducing light.

Under the action of the joint field of two recording beams (1), the corresponding complex birefringence is induced in the recording material, which is described by the Jones matrix [8]. In this case the following expressions were obtained for Jones matrix

$$M = M_0 + M_{-1} + M_{+1}, \tag{3}$$

where

$$M_0 \approx \exp(-2i\kappa d\hat{n}_0) \begin{pmatrix} 1 & 0 \\ 0 & 1 \end{pmatrix}, \tag{4}$$

$$M_{-1} \approx -\frac{i\kappa d}{2\hat{n}_o} \exp(-2i\kappa d\hat{n}_0) \exp(i\delta) \times \begin{pmatrix} (\hat{s} + \hat{v}_L)\hat{\psi}_x^* \hat{\xi}_x + (\hat{s} - \hat{v}_L)\hat{\psi}_y^* \hat{\xi}_y & (\hat{v}_L + \hat{v}_G)\hat{\psi}_x^* \hat{\xi}_y + (\hat{v}_L - \hat{v}_G)\hat{\psi}_y^* \hat{\xi}_x \\ (\hat{v}_L - \hat{v}_G)\hat{\psi}_x^* \hat{\xi}_y + (\hat{v}_L + \hat{v}_G)\hat{\psi}_y^* \hat{\xi}_x & (\hat{s} - \hat{v}_L)\hat{\psi}_x^* \hat{\xi}_x + (\hat{s} + \hat{v}_L)\hat{\psi}_y^* \xi_y \end{pmatrix}, \tag{5}$$

$$M_{+1} \approx -\frac{i\kappa d}{2\hat{n}_o}\exp(-2i\kappa d\hat{n}_0)\exp(-i\delta) \times \begin{pmatrix} (\hat{s}+\hat{v}_L)\hat{\psi}_x\hat{\xi}_x^* + (\hat{s}-\hat{v}_L)\hat{\psi}_y\hat{\xi}_y^* & (\hat{v}_L+\hat{v}_G)\hat{\psi}_y\hat{\xi}_x^* + (\hat{v}_L-\hat{v}_G)\hat{\psi}_x\hat{\xi}_y^* \\ (\hat{v}_L-\hat{v}_G)\hat{\psi}_y\hat{\xi}_x^* + (\hat{v}_L+\hat{v}_G)\hat{\psi}_x\hat{\xi}_y^* & (\hat{s}-\hat{v}_L)\hat{\psi}_x\hat{\xi}_x^* + (\hat{s}+\hat{v}_L)\hat{\psi}_y\hat{\xi}_y^* \end{pmatrix} \quad (6)$$

Here $\kappa = 2\pi/\lambda$; λ is the wavelength, and d is the thickness of the medium. Matrix M_0 in (4) is responsible for forming the nondiffracted order, matrices M_{-1} and M_{+1} are, respectively, responsible for forming orders -1 and +1.

With (5) and (6) it is easy to obtain Jones matrices of gratings for different combinations of the polarization state of recording beams. Substituting into (5) and (6) the concrete values of the components of the Jones vectors of the recording beams and the characteristics of the recording medium, we can obtain matrices M_{-1} and M_{+1} for different type of polarization-holographic gratings using recording media with different characteristics.

Currently, we use three polarization-holographic gratings for creation the polarization-holographic element: grating recorded by orthogonal circularly polarized beams (grating *C*); grating recorded by two parallel vertically linearly polarized beams (grating L_{90}) and grating recorded by two parallel linearly polarized beams with an azimuth of linear polarization of 45^0 (grating L_{45}). At present we use +1 and -1 orders from grating C and +1 orders from gratings L_{90} and L_{45}. This configuration enables to completely circumvent the distortions of the polarization state caused by the imperfection of the recording material [3].

It follows from (5) and (6) that the Jones matrices responsible for formation diffraction orders by each grating are written in the form [4]:

$$\begin{aligned} M_{\mp1,C} &\approx A\frac{\psi_C^2}{2}\exp[\mp i(a_x-b_x)]\exp(\pm i\delta)\begin{pmatrix}1 & \mp i\\ \mp i & -1\end{pmatrix} \\ M_{\mp1,C} &\approx A\frac{\psi_C^2}{2}\exp[\mp i(a_x-b_x)]\exp(\pm i\delta)\begin{pmatrix}1 & \mp i\\ \mp i & -1\end{pmatrix} \\ M_{\mp1,90} &\approx A\frac{\psi_{90}^2}{2}\exp[\mp i(a_y-b_y)]\exp(\pm i\delta)\begin{pmatrix}0 & 0\\ 0 & 1\end{pmatrix} \\ M_{\mp1,45} &\approx A\frac{\psi_{45}^2}{2}\exp[\mp i(a_x-b_x)]\exp(\pm i\delta)\begin{pmatrix}1 & 1\\ 1 & 1\end{pmatrix} \end{aligned} \quad (7)$$

where $A = -\frac{i\kappa d\hat{v}_L}{2\hat{n}_o}\exp(-2i\kappa d\hat{n}_0)$.

Let us a beam with the Jones vector $\begin{pmatrix}E_x\exp i\varepsilon_x\\ E_y\exp i\varepsilon_y\end{pmatrix}$ incomes on the element and diffracts on them.

The Jones vectors of diffracted orders are derived from multiplication of the Jones matrices responsible for the formation of appropriate diffraction order by the Jones vector of the incoming wave. As a result, we have obtained the Jones vectors of the beams diffracted on the element and the corresponding intensities of the diffracted orders have the following form

$$\begin{aligned} I_{-1,C} &\approx \frac{1}{2}A^2\psi_C^4[E_x^2+E_y^2-2E_xE_y\sin(\varepsilon_y-\varepsilon_x)] \\ I_{+1,C} &\approx \frac{1}{2}A^2\psi_C^4[E_x^2+E_y^2+2E_xE_y\sin(\varepsilon_y-\varepsilon_x)] \\ I_{-1,L_{90,45}} &\approx A^2\psi_L^4[E_x^2+E_y^2+2E_xE_y\cos(\varepsilon_y-\varepsilon_x)] \\ I_{+1,L_{90,45}} &\approx \frac{1}{2}A^2\psi_L^4E_y^2, \end{aligned} \quad (8)$$

where $A^2 = \left(\frac{\kappa d}{2n_0}\right)^2$ and $\kappa = \frac{2\pi}{\lambda}$, λ - element recording wavelength, d- thickness of the light-sensitive layer, n_0 - refractive index of the recording material, ψ_C^2, ψ_L^2 - recording beams intensities; E_x, E_y - amplitudes and ε_x, ε_y - the phases of the incoming beam along the *x* and *y* axes, respectively.

The light beam incomes onto the polarization-holographic element, diffracts on them and the simultaneous measurement of the intensities of four diffracted beams enables all the four Stokes parameters to be determined.

We have obtained formulas for the Stokes parameters depending on the intensities of the beams diffracted on the element in each point (x, y) of the images of an object taking into account also the dispersion of the polarization state due to the angular dispersion of an element.

The relationship between the Stokes parameters and the diffraction orders intensities was obtained in the form [4]

$$\begin{aligned} S_{0,\lambda_i} &= k_{C,\lambda_i}(I_{+C}+I_{-C}) \\ S_{1,\lambda_i} &= k_{C,\lambda_i}(I_{+C}-I_{-C}) - 2k_{90,\lambda_i}I_{90} \\ S_{2,\lambda_i} &= 2k_{45,\lambda_i}I_{45} - k_{C,\lambda_i}(I_{+C}-I_{-C}) \\ S_{3,\lambda_i} &= k_{C,\lambda_i}(I_{+C}-I_{-C}) \end{aligned} \quad (9)$$

Here I_{+C} and I_{-C} are intensities of +1st and -1st orders from grating C; I_{90} and I_{45} are intensities of +1st order from gratings L_{90} and L_{45}, accordingly. Coefficients $k_{90,\lambda i}$, $k_{45,\lambda i}$, $k_{C,\lambda i}$ are connected with absorption of light in an element, the diffraction efficiency of an element, wavelength and the optoelectronic transformations by a photodetector. The values of these coefficients are determined experimentally during calibration of the sensor.

Fig. 1 shows schematic picture of diffraction on the element.

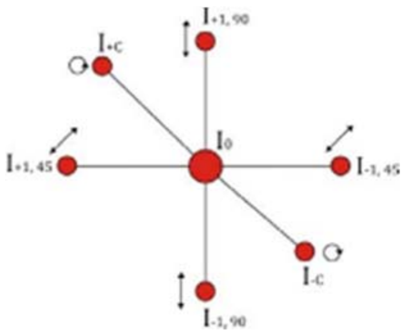

Fig. 1. Schematic picture of diffraction on the element.

We can determine all the four Stokes parameters by simultaneous measurement of the intensities of diffracted orders by using photometric scheme.

The corresponding parameters of the polarization ellipse can be determined:

the ellipticity, $\varepsilon = \dfrac{S_3}{1+\sqrt{{S_1}^2+{S_2}^2}}$;

the azimuth of light $\alpha = \dfrac{1}{2} arctg \dfrac{S_2}{S_1}$ and

the degree of polarization $DOP = \dfrac{\sqrt{S_1^2+S_2^2+S_3^2}}{S_0}$.

The polarization-holographic diffraction element gives the possibility for real-time determination of the point-by-point distribution of the polarization state in the image of an object by using the appropriate software. We can take into account also the dispersion of the polarization state due to the angular dispersion of an element, which provides additional information.

To measure the intensity distribution in the diffracted orders, a photodetector matrix (such as CCD) is used, the sensitivity and dynamic range of which are selected in accordance with a specific task.

On Fig. 2 an optical scheme of the polarization state sensor is shown.

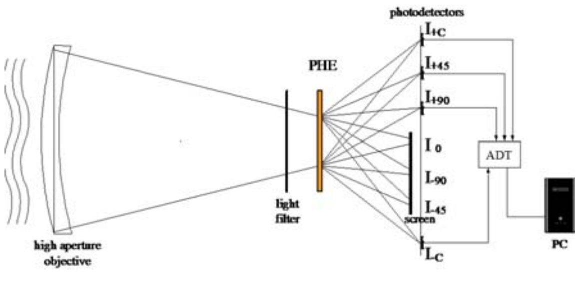

Fig. 2. Optical scheme of the polarization state sensor.

In Fig. 2, the objective forms an object image in the plane of the CCD matrix. In front of the focal plane of the objective, a polarization-holographic element is placed, which forms the diffraction orders. Each diffraction order contains an image of the object under study. Special software has been developed for point-to-point comparison of the intensities of images in diffracted beams, which enables to obtain the polarization state distribution over the object surface without any scanning.

The objective, polarization-holographic element. CCD camera and software represent *the polarization state sensor* [13].

This sensor connected to the computer with the software is a quasi-real time imaging Stokes spectropolarimeter. The sensor speed depends on the exposure of the CCD camera and on the computer processing time. For most sensor applications, the time of obtaining the polarization state distribution over an object image is units or tens of milliseconds.

Besides when narrow-band filters are used, these allow to obtain the dispersion of the distribution of the polarization state in the images of the objects for any wavelengths from a working range of the element 500 – 1600 nm.

Since the optical system consists an objective and the polarization-holographic element, there is practically no internal reflections of light, which significantly reduces the distortion of the polarization state of light under investigation and thereby reduces instrumental error.

Fig. 3 shows experimental and theoretical value variations of all Stokes parameters obtained by means of monochromatic source of linearly polarized light with change in azimuth with step of 5 degrees over the range of 0-360 degrees. These curves were obtained for light beam of a He-Ne laser (632.8 nm, power 3 mW). We see good agreement between the experimental and theoretical curves for all four Stokes parameters. Similar curves were obtained for a wavelength of 532 nm using different powers from 1 to 20 mW, as well as for infrared radiation of 1.15 μm. According to our estimate, the accuracy of the single experimental determination of the Stokes parameters is about 0.1 %. The sensitivity of the sensor depends on the sensitivity of the CCD camera, and at high exposures for very dim objects (for example, in astropolarimetry), the speed is greatly reduced and ranges from a few to tens of seconds.

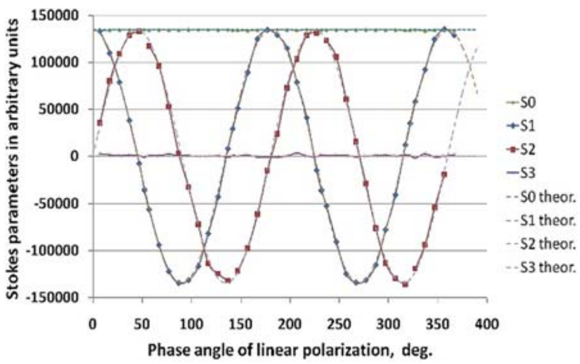

Fig. 3. Experimental and theoretical value variations of all 4 Stokes parameters.

We have obtained integral polarization-holographic elements with working spectral range from 500 nm to 1600 nm, a working aperture can be from 0.5 cm up to 5 cm in diameter and with a total diffraction efficiency of the element at wavelength of 532 nm close to 75 %, 635 nm close to 60 %, 1150 nm close to 20 %, and 1550 nm close to 8 %.

For recording the element, a polarization-sensitive material was used on the basis of azo dye Pure Mordant Yellow (PMY) modified by us and a gelatin matrix which was specially processed to increase the stability of the polarization-holographic element. The optical density of the material was approximately 2.2 at the wavelength of recording (473 nm), and the thickness of the emulsion layer was about 20 microns. Energy exposure was about 50 J/cm^2 for recording each grating.

Calibration is necessary to determine the coefficients for each element and photodetectors. As experiments have shown, it is most convenient to carry out this calibration by non-polarized quasi-monochromatic light from a point source of unpolarized light, giving a homogeneous intensity distribution in a large solid angle (a so-called "artificial star"). We used narrow-band interference filters for wavelengths of 532 nm and 635 nm with transmission band of 10 nm.

To determine the coefficients in (9), we must measure the values of intensities $I_{+1,C}$, $I_{-1,C}$, $I_{+1,90}$, $I_{+1,45}$ in the plane of localization of the diffraction orders. Than we select the order with the highest intensity, for example, $I_{+1,C}$. Coefficients k_λ are determined for the given wavelength as follows

$$k_{-1,C} = \frac{I_{+1,C}}{I_{-1,C}},\quad k_{+1,45} = \frac{I_{+1,C}}{I_{+1,45}},\quad k_{+1,90} = \frac{I_{+1,C}}{I_{+1,90}} \tag{10}$$

Validation of the element was carried out by laser beams of wavelength 532 nm and 635 nm with test polarizations: left circularly polarized, linearly polarized with azimuths from -20 degrees up to +200 degrees with steps of 5 degrees and the polarization degree close to 100 %. By taking into account the obtained coefficients k_λ the photometric scheme must give us the Stokes parameters corresponding to the used polarization state when the polarization degree is close to 100 %.

The experiments showed that measurements error for intensities of the diffracted orders is 0.1 % with a single measurement and this corresponds to 0.2 % in determining the Stokes parameters. However, the software provides for the averaging of 50 single measurements, which are carried out for 0.5 s, and the relative measurement error of the intensities is about 0.002 %, and for the Stokes parameters - 0.004 %. The measurement accuracy of the degree of polarization is of about 0.15 %, and an accuracy of an azimuth of linear polarization of about 40 angular minutes.

For one of the element and photodetector matrix from camera Canon EOS 5D with CCD of 36 × 25 mm the following values of the coefficients was obtained by using the described method: for wavelength of 635 nm $k_{+1,90} = 1$, $k_{+1,45} = 1{,}346$, $k_{-1,C} = 8{,}553$, $k_{+1,C} = 7{,}916$ and for 532 nm $k_{+1,90} = 1$, $k_{+1,45} = 1{,}287$, $k_{-1,C} = 8{,}135$, $k_{+1,C} = 7{,}625$.

3. Polarization State Sensor Applications

We tested this sensor in the tasks of astropolarimetry, remote sensing, pattern recognition, for determining the stress state distribution in various constructions [14, 15].

3.1. Application in Remote Sensing

Natural light is more or less polarized while reflected from the surface of objects. The state and degree of polarization of reflected and scattered light depend on the physicochemical properties of the surface from which light is reflected, also on the angle of incident light. Information about the state of polarization can make a considerable contribution to the classification of materials and identification of objects and, together with the existing methods of recognition can significantly raise the accuracy of identification during remote sensing [16].

Current models of determining information by using the function BRDF are well enough developed, and the approximate models are used for determining distribution of the polarization state. However these approaches are difficult [17, 18].

We have developed a spectro-polarimetric method by means of the analysis of the distribution of state and degree of polarization of light reflected from a recognizable object, in which the polarization state sensor is used for a full analysis of the polarization state. The polarization state of light reflected from the object enables to obtain the physical-chemical characteristics of the object surface [19].

According to the theoretical model developed by us it is possible to determine optical characteristics of the material of the surface of an object by the values of the Stokes parameters in the images of objects using the Jones matrix of the anisotropic surface and one angle of observation and incidence [19].

Experimentally the possibility of obtaining the distribution of values of the Stokes parameters on the image of objects was shown for objects from different materials and of a different geometric form.

Software has been developed for the point-by-point definition of the Stokes parameters in the images of objects, as well as it giving the possibility to obtain average values of the Stokes parameters on the images in a solid angle close to the direction of specular reflection. As an example, Fig. 4 shows the program interfaces for objects of a round form made from copper and organic glass for the red spectral region (spectral maximum 630 nm).

Investigation of the dispersion of the Stokes parameters was carried out on the same objects. The experiments showed a significant difference both in the point-by-point distribution of the values of the Stokes parameters and in their average values, also in values of dispersion of the average Stokes parameters for green and red spectral region. The value of average dispersion $\nu = S_{i,G} - S_{i,R}$, where $S_{i,G}$ and $S_{i,R}$ are the averaged Stokes parameters for green (530 nm) and red spectral region (630 nm), respectively: for copper ν_{S1} = 0.468759, ν_{S2} = -0.041721, ν_{S3} = 0.067166; for organic glass ν_{S1} = 0.224136, ν_{S2} = 1,068955, ν_{S3} = 0.038019.

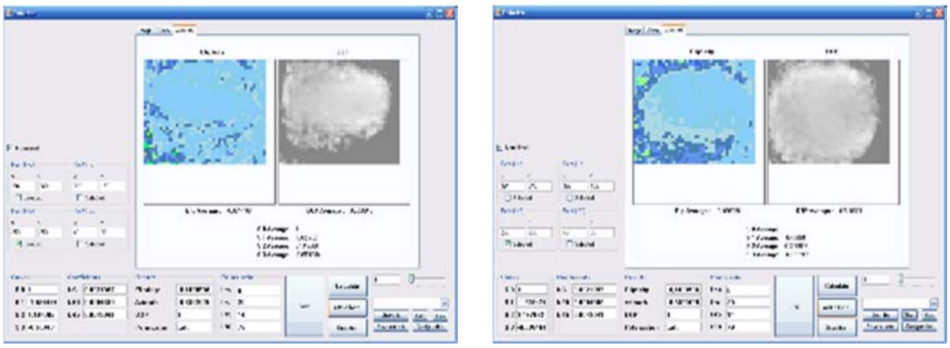

Fig. 4. Program interfaces for objects from copper (on left) and organic glass (on right) for the red spectral region and for the angle of illumination of 40^0 and angle of observation of 50^0.

This method significantly improves the recognition of various objects. The method works both in natural lighting of the object and in the case of artificial lighting.

We have developed a spectro-polarimetric method by means of the analysis of the distribution of state and degree of polarization of light reflected from a recognizable object, in which the polarization state sensor is used for a full analysis of the polarization state [19].

3.2. Stress-state Distribution in Different Constructions

The problem of quantitative determining the stress distribution in different detailes and constructions is solved by various methods: tensometry, the X-ray method, the magnetic methods, the method of acoustoelasticity, *et al.*

The method of holographic interferometry allows a picture of stress distribution to be obtained on the surface of a construction, but it is very critical to the conditions of carrying out an experiment and the interpretation of the obtained interference pattern is quite complicated. In addition, this method does not allow the results to be obtained in real time. Although the modern digital methods of holographic interferometry are more convenient and fast, they however require a comparison of a stressed state with a stress-free one, the illumination by coherent light and are also critical to the conditions of an experiment [20, 21].

In general, these methods do not work in real time, are rather time-consuming and have limitations on the materials and type of loads.

The polarization-optical method of stress analysis (a method of photoelasticity) enables the stress distribution in various constructions and details to be obtained, but it involves making the transparent models of these constructions from the materials having photoelasticity or gluing the plates from these materials on the construction under investigation, which limits the application field and reduces the measurement accuracy [22].

Despite the variety of the currently available various methods for the determination of stresses, the development of a non-destructive, technological, sensitive, convenient, all-purpose and real-time method for determining the distribution of the stress states over a wide area is extremely urgent.

It is known that mechanical stress in solids causes change in the permittivity tensor, and this change leads to the occurrence of optical anisotropy, in particular, to the occurrence of birefringence. The polarization state of the light reflected from the surface of the object or transmitted through it is the most sensitive to changes of optical properties and the determination of changes in the polarization state in the presence of stresses in solids will enable a quantitative relationship between the magnitudes of the stresses and changes in the polarization state to be established. The known stress-optic law gives the ratio between the change in the refractive index and stresses. The values of the Stokes parameters enables the value of stress to be determined at each point of the object surface. The theoretical model is presented in [23].

We have developed a real time polarimetric method for stress measurement by means of the analysis of the distribution of the state and degree of polarization of light reflected from a stressed object by use the polarization state sensor [24]. We have developed and created an appropriate laboratory model of the set-up which consists the unit for creating the dosated stresses in samples of various materials and the optical scheme based on the polarization state sensor.

There was the possibility of creating the uniaxial stresses in the sample from 0 to 125 MPa in increments of 12.5 MPa. A device with a controlled force was constructed on the basis of hydraulic jacks to create the uniaxial and biaxial dosated stresses in sample No. 5. The maximum stress in the sample were 4.9×10^8 N/m^2 in the vertical direction and 2.94×10^8 N/m^2 in the horizontal direction. In this device the possibility exists for the installation of the samples of different sizes: from 5×4 cm to 15×12 cm.

Light from the illuminator is incident on an object and reflected from it. As an illuminator, projectors based on halogen or xenon lamps, and also laser sources with wavelengths of 635 nm and 532 nm can be used. In the case of using white light, narrowband interference filters are installed in the scheme before the polarization holographic element to eliminate the influence of the angular dispersion of the element, distorting the images in the diffracted orders. The object was illuminated at an angle close to 45 degrees to the normal to the sample surface, and the observation was carried out in the direction of maximum indicatrix of the scattering from the object surface at an angle close to –45 degrees. By means of the specially developed software, we get an image of distribution of the polarization state and also of the stressed state of a source material.

We investigated samples of 8 × 10 × 5 cm of the following materials: untempered steel 45, grade of concrete 400, red brick, technical aluminum, duralumin D16. The surface of the samples was ground by fine sandpaper and surface roughness was almost the same for all samples. The samples were illuminated sequentially by a laser beam with a wavelength of 635 nm and 532 nm, with the right circularly and linearly polarized radiation with an azimuth of 0 degree. For experimental determination of the stress state distribution for different dosated load for a given material of the object we have determined the distribution of the values of the Stokes parameters and the corresponding values of the degree of polarization and ellipticity of the polarization ellipse of the light reflected from the sample surface.

As an example, Fig. 5 shows the dependence of the degree of polarization on the stress in three samples: steel 45, concrete grade 400 and aluminum in case of illuminating the sample with a laser beam of 635 nm.

As follows from these curves there is a significant difference for the samples from different materials. So, for a sample of steel the degree of polarization increases monotonically with increasing the stress (there is a small plateau due to the start of yielding flow of the material at 50 - 80 MPa), and then the rise is observed again. In case of concrete the increase in the degree of polarization is observed under certain loads (at 20-50 MPa). With the further increase of stresses, the degree of polarization increases and then the recession of the values of the degree of polarization begins at 90-110 MPa, which obviously is due to the formation of microcracks. For aluminum, there is almost a constant value of the degree of polarization for all loads, due to its high plasticity.

By means of the laboratory model, we have investigated the possibility of determining the distribution of stressed state on the surface of the object, including diffuse reflecting objects. As an example, Fig. 6 demonstrates screenshots showing the change in the polarization state of light reflected from the object surface (steel ingot by the size of 7×5×5 cm) with application of load perpendicular to the length.

The screenshots show a picture without a load, and with a load of 20 kN and 40 kN. On the right of each screenshots, the color scales are shown in which each color corresponds to the definite load values. The figures show that the picture changes significantly when the load is applied.

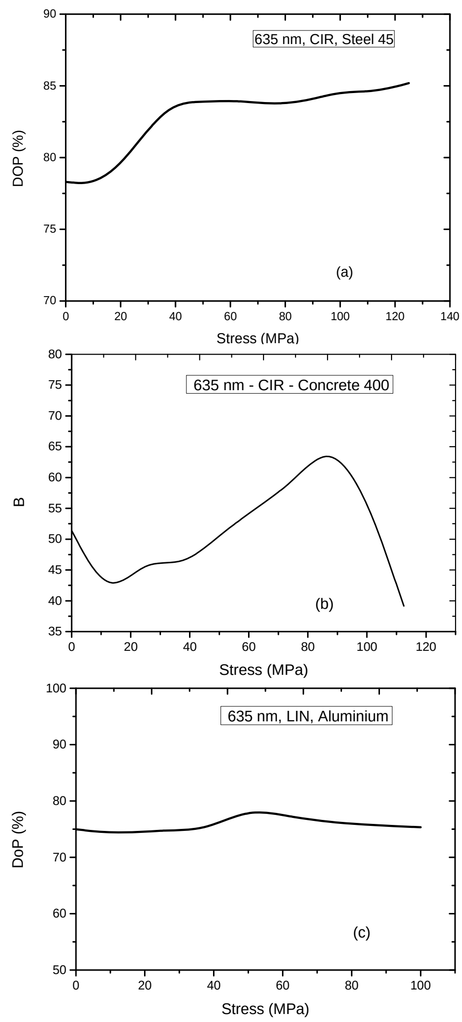

Fig. 5. The dependence of the degree of polarization on the stress in three samples of: (a) steel 45; (b) concrete grade 400; (c) aluminum. Illuminating by laser beam of 635 nm.

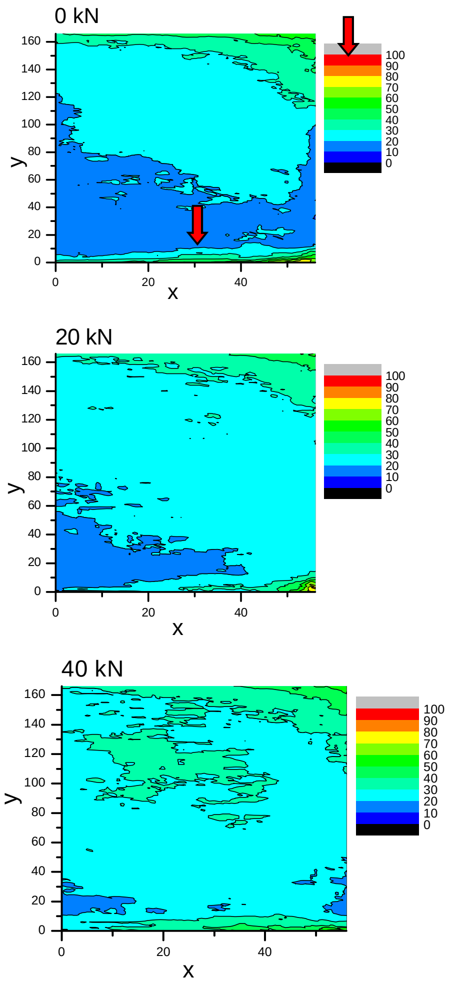

Fig. 6. The distribution of the stress states in the sample of steel 45 in case of different loads: 0, 20, 40 kN.

This approach seems very promising because, unlike the existing methods, it does not require the creation of transparent models of objects or sticking plates from transparent photoelastic materials on an object and also it does not require double-exposure holographic registration of an object and it is extremely sensitive. The method is nondestructive, i.e. there is no need to drill holes or openings in the product to determine the residual stresses. This method will enable the monitoring and diagnosis of already existing constructions to be carried out.

4. Conclusions

The real time complete analysis of polarization state of light is suggested by means of polarization state sensor based on the polarization-holographic elements. Such a polarization state sensor has many advantages compared to conventional devices of polarization optics: it enables to carry out the polarization analysis and transformation of light in real time; operate in a wide spectral range and do not require making mechanical moving and rotations or tuning of electronic units in working process. It differ by compactness, universality, simplicity, light weight, high speed and comparative cheapness.

Besides, the use of a polarization state sensor allows the distortion of the polarization state to be eliminated which inevitably appears when using sequentially several polarization-holographic gratings, and also in polarimeters of other types.

The polarization state sensor can also be applied to machine vision, for example, in autonomous cars and drones.

Acknowledgements

Authors gratefully acknowledge the Shota Rustaveli National Science Foundation of Georgia support by the grant № AR-19-1154.

References

[1]. Sh. Kakichashvili, On polarization recording of holograms, *Optics and Spectroscopy,* Vol. 33, Issue 2, 1972, pp. 324-327 (in Russian).

[2]. Sh. Kakichashvili, Polarization holography, *Nauka, Leningrad,* 1989 (in Russian).

[3]. B. Kilosanidze, G. Kakauridze, Polarization-holographic gratings for analysis and transformations of light: 1. The analysis of completely polarized light, *Applied Optics*, Vol. 46, 2007, pp. 1040-1049.

[4]. G. Kakauridze, B. Kilosanidze, Polarization-holographic diffraction element-based real-time Imaging Stokes spectropolarimetry, in *Proceedings SPIE of the Symposium Photonics West,* San Francisco, USA, Vol. 7957, 22-28 January 2011, pp. 22-28.

[5]. L. Kaiser, E. Frins, B. Hils, L. Beresnev, W. Dultz, H. Schmitzer, Polarization analyzer for all the states of polarization of light using a structured polarizer, *Journal of the Optical Society of America A,* Vol. 30, 2013, pp.1256-1260.

[6]. I. Moreno, J. A. Davis, K. Badham, *et al.,* Vector Beam Polarization State Spectrum Analyzer, *Scientific Reports*, Vol. 7, Issue 1, 2017, 2216.

[7]. B. Kilosanidze, G. Kakauridze, Polarization-holographic diffraction element for complete analysis of light, in *Proceedings SPIE of the Optics + Optoelectronics Symposium,* Prague, Czech Republic, Vol. 7358, 20-22 April 2009, pp. 7358A.

[8]. Jones R. C., A new calculus for the treatment of optical systems, *Journal of the Optical Society of America,* Vol. 31, 1941, pp. 488-493.

[9]. Sh. Kakichashvili, B. Kilosanidze, V. Shaverdova, Anisotropy and gyrotropy of dye mordant pure-yellow Induced by linear polarized light, *Optics and Spectroscopy*, Vol. 68, 1990, pp. 1309-1312 (in Russian).

[10]. I. Chaganava, G. Kakauridze. B. Kilosanidze, G. Datukishvili, Development of high- performance, stable and moisture-resistant polarization-sensitive materials, in *Proceedings SPIE of the Optical Engineering + Applications Symposium,* San Diego CA, USA, Vol. 8126, 21-25 Aug. 2011, pp. 1-10.

[11]. Sh. Kakichashvili, On the regularity in photoanisotropic phenomena, *Optics and Spectroscopy*, Vol. 52, 1982, pp. 317-322 (in Russian).

[12]. Sh. Kakichashvili, On the regularity in the phenomena of photoanisotropy and photogyrotropy, *Optics and Spectroscopy*, Vol. 63, 1987, pp. 911-917 (in Russian).

[13]. B. Kilosanidze, G. Kakauridze, Polarization state sensor, in *Proceedings of the 4th International Conference on Optics, Photonics and Lasers (OPAL' 2021),* Corfu, Greece, 13-15 October 2021, pp. 145-149.

[14]. G. Kakauridze, B. Kilosanidze, T. Kvernadze, G. Kurkhuli, Astropolarimetry with a Polarization-holographic Imaging Stokes Polarimeter, *Journal of Astronomical Telescopes, Instruments, and Systems JATIS*, Vol. 5, Issue 1, 2019, 015002.

[15]. B. Kilosanidze, G. Kakauridze, I. Kobulashvili, Pattern recognition system based on photoanisotropic copies, *Applied Optics*, Vol. 58, Issue 7, 2019, pp. 1778-1788.

[16]. S. R. Cloude, Polarization. Applications in remote sensing, *Oxford University Press Inc.*, New York, 2010.

[17]. J. Schott, Fundamentals of polarimetric remote sensing, *SPIE Press,* Bellingham, Washington, 2009.

[18]. J. S. Tyo, D. L. Goldstein, D. B. Chenault, J. A. Shaw, Review of passive imaging polarimetry for remote sensing applications, *Applied Optics*, Vol. 45, Issue 22, 2006, pp. 5453-5469.

[19]. B. Kilosanidze, G. Kakauridze, Determination of the characteristics of the surface of objects at optical remote sensing by the Polarization-Holographic Imaging Stokes Spectro-polarimeter, in *Proceedings of the SPIE Optical Metrology, Co-located with Laser World of Photonics,* Munich, Germany, Vol. 8082, 23-26 May 2011, pp. 8082-126.

[20]. R. Jones, C. Wykes, Holographic and Speckle Interferometry, *Cambridge University Press*, 1989.

[21]. G. Pedrini, P. Fröning, H. Fessler, H. J. Tiziani, In-line digital holographic interferometry, *Applied Optics*, Vol. 37, 1998, pp. 6262-6269.

[22]. J. Dijkstra, W. Broere, New method of full-field stress analysis and measurement using photoelasticity, *Geotechnical Testing Journal*, Vol. 33, Issue 6, 2010, pp. 6-20.

[23]. G. Kakauridze, B. Kilosanidze, T. Kvernadze, G. Kurkhuli, A new real-time polarimetric method for determining the distribution of stressed state in different constructions, *Proceedings Photonic Instrumentation Engineering II SPIE OPTO, S*an Francisco, USA, 22-28 January, Vol. 9369, 2015, pp. 9369OU1-10.

[24]. B. Kilosanidze, G. Kakauridze, T. Kvernadze, G. Kurkhuli, Sensor for real-time determining the polarization state distribution in the object images, in *SPIE Proceedings of the Symposium Optics and Photonics for Counterterrorism, Crime Fighting, and Defence XI,* Toulouse, France, Vol. 9652, 23-27 September 2015, p. 96520M1-10.